Dentate gyrus volume deficit in schizophrenia

Soichiro Nakahara[1,2], Jessica A. Turner[3,4,5], Vince D. Calhoun[3,5,6,7], Kelvin O. Lim[8], Bryon Mueller[8], Juan R. Bustillo[7], Daniel S. O'Leary[9], Sarah McEwen[10], James Voyvodic[11], Aysenil Belger[12], Daniel H. Mathalon[13,14], Judith M. Ford[13,14], Fabio Macciardi[15], Mitsuyuki Matsumoto[2], Steven G. Potkin[15] and Theo G. M. van Erp[1,16]

[1]Clinical Translational Neuroscience Laboratory, Department of Psychiatry and Human Behavior, University of California Irvine, Irvine, CA 92617, USA; [2]Virtual Venture Unit, Psychiatry, Drug Discovery Research, Astellas Pharma Inc., 21, Miyukigaoka, Tsukuba, Ibaraki 305-8585, Japan; [3]The Tri-institutional Center for Translational Research in Neuroimaging and Data Science (TReNDS) {Georgia State, Georgia Tech, Emory}, Atlanta, GA 30300, USA; [4]Departments of Psychology and Neuroscience, Georgia State University, Atlanta, GA 30302, USA; [5]Mind Research Network, Albuquerque, NM 87106, USA; [6]Department of Electrical and Computer Engineering, University of New Mexico, Albuquerque, NM 87131, USA; [7]Departments of Psychiatry & Neuroscience, University of New Mexico, Albuquerque, NM 87131, USA; [8]Department of Psychiatry, University of Minnesota, Minneapolis, MN 55454, USA; [9]Department of Psychiatry, University of Iowa, Iowa City, IA 52242, USA; [10]Department of Psychiatry, University of California, San Diego, La Jolla, CA 92093, USA; [11]Brain Imaging and Analysis Center, Duke University Medical Center, Durham, NC 27710, USA; [12]Department of Psychiatry, University of North Carolina at Chapel Hill, Chapel Hill, NC 27599, USA; [13]Department of Psychiatry, Weill Institute for Neurosciences, University of California, San Francisco, San Francisco, CA 94143, USA; [14]Veterans Affairs San Francisco Healthcare System, San Francisco, CA 94121, USA; [15]Department of Psychiatry and Human Behavior, University of California Irvine, Irvine, CA 92617, USA and [16]Center for the Neurobiology of Learning and Memory, University of California Irvine, Irvine, CA 92697, USA

Abstract

Background. Schizophrenia is associated with robust hippocampal volume deficits but sub-region volume deficits, their associations with cognition, and contributing genes remain to be determined.

Methods. Hippocampal formation (HF) subregion volumes were obtained using FreeSurfer 6.0 from individuals with schizophrenia ($n = 176$, mean age ± S.D. = 39.0 ± 11.5, 132 males) and healthy volunteers ($n = 173$, mean age ± S.D. = 37.6 ± 11.3, 123 males) with similar mean age, gender, handedness, and race distributions. Relationships between the HF sub-region volume with the largest between group difference, neuropsychological performance, and single-nucleotide polymorphisms were assessed.

Results. This study found a significant group by region interaction on hippocampal subregion volumes. Compared to healthy volunteers, individuals with schizophrenia had significantly smaller dentate gyrus (DG) (Cohen's $d = -0.57$), Cornu Ammonis (CA) 4, molecular layer of the hippocampus, hippocampal tail, and CA 1 volumes, when statistically controlling for intracranial volume; DG ($d = -0.43$) and CA 4 volumes remained significantly smaller when statistically controlling for mean hippocampal volume. DG volume showed the largest between group difference and significant positive associations with visual memory and speed of processing in the overall sample. Genome-wide association analysis with DG volume as the quantitative phenotype identified rs56055643 ($\beta = 10.8$, $p < 5 \times 10^{-8}$, 95% CI 7.0–14.5) on chromosome 3 in high linkage disequilibrium with *MOBP*. Gene-based analyses identified associations between *SLC25A38* and *RPSA* and DG volume.

Conclusions. This study suggests that DG dysfunction is fundamentally involved in schizophrenia pathophysiology, that it may contribute to cognitive abnormalities in schizophrenia, and that underlying biological mechanisms may involve contributions from *MOBP*, *SLC25A38*, and *RPSA*.

Introduction

The hippocampal formation (HF) is among the brain structures that show the most robust volume deficits in schizophrenia (Haijma *et al.*, 2013; Okada *et al.*, 2016; van Erp *et al.*, 2016) though subregion abnormalities, relationships with cognitive performance, and contributing genetic loci remain to be determined. Regional HF abnormalities have been hypothesized and observed (Schobel *et al.*, 2009; Tamminga *et al.*, 2010, 2012; Small *et al.*, 2011). Tamminga *et al.* hypothesized that a primary deficit in the hippocampal dentate gyrus (DG) disrupts memory presentations in schizophrenia (Tamminga *et al.*, 2010), while Small *et al.* hypothesized that a primary deficit in Cornu Ammonis (CA) 1 disrupts memory integration in schizophrenia (Small *et al.*, 2011). The HF's trisynaptic circuit includes subregions

CAMBRIDGE
UNIVERSITY PRESS

that subserve different functions and differ in cellular make-up, e.g. the principal cell type in the DG is the granule cell and in the CA the pyramidal cell (Amaral and Witter, 1989; Amaral *et al.*, 2007; Small *et al.*, 2011; Wheeler *et al.*, 2015; Nakahara *et al.*, 2018). Hence, different biological mechanisms may contribute to HF subregion volume abnormalities observed in schizophrenia.

Several automated HF segmentation methods exist (Van Leemput *et al.*, 2008, 2009; Yushkevich *et al.*, 2009; Iglesias *et al.*, 2013; Adler *et al.*, 2014). Two of these methods (Van Leemput *et al.*, 2008, 2009; Iglesias *et al.*, 2013) are implemented in FreeSurfer (Fischl *et al.*, 2002; Fischl, 2012) and have been most widely used in schizophrenia studies. Subregions shown to have lower volume in schizophrenia compared to controls include the CA1 (Hýža *et al.*, 2016; Ho *et al.*, 2017a, 2017b; Ota *et al.*, 2017; Sauras *et al.*, 2017), CA2/3 (Ho *et al.*, 2017a, 2017b), DG (Ho *et al.*, 2017b; Ota *et al.*, 2017), and the subiculum (Francis *et al.*, 2013; Mathew *et al.*, 2014; Haukvik *et al.*, 2015). These findings suggest that regional deficits in DG-CA3-CA1-subiculum circuitry may contribute to the emergence of psychosis (Yushkevich *et al.*, 2008, 2009; Van Leemput *et al.*, 2009).

Most schizophrenia HF subregion studies employed FreeSurfer 5.1–5.3; (Haukvik *et al.*, 2018; Nakahara *et al.*, 2018), for which limitations have been reported (Wisse *et al.*, 2014). Hitherto, only two schizophrenia studies assessed HF subregion volumes using FreeSurfer 6.0's improved *ex vivo* hippocampal subregion atlas segmentations (Iglesias *et al.*, 2013) run on FreeSurfer 5.3 whole hippocampus segmentations (Ho *et al.*, 2017a, 2017b). Ho *et al.* found a progressive decline in CA1 volume in individuals at risk for psychosis (Ho *et al.*, 2017a) and more widespread volume deficits and progressive decline in DG and CA3 after illness onset (Ho *et al.*, 2017b). To our knowledge, only one schizophrenia study has reported HF subregion volumes obtained using only FreeSurfer 6.0 (Baglivo *et al.*, 2017). A major advantage of FreeSurfer 6.0 is that its *ex vivo* atlas provides separate DG and CA4 volume estimates (Iglesias *et al.*, 2013). This distinction is important for testing Tamminga *et al.*'s hypothesis (Tamminga *et al.*, 2010) because it focuses on the DG and CA3 but not CA4. Moreover, given that no study to date has tested for a group by region interaction on HF subregion volumes, the possibility of differential regional HF volume abnormalities remains untested.

Schizophrenia is a heritable and HF subregion volume heritabilities are estimated at 40–70% (Greenspan *et al.*, 2016; Whelan *et al.*, 2016), suggesting that genetic variation may contribute to psychosis-related HF abnormalities. However genetic mechanisms contributing to HF subregion volume deficits remain undetermined.

In this study, we compared HF subregion volumes obtained using FreeSurfer 6.0 between 176 individuals with schizophrenia and 173 healthy volunteers recruited into the Function Biomedical Informatics Research Network (FBIRN) Phase 3 study. We tested for a group by region interaction on regional volumes and computed group contrast effect sizes. Based on our review of the literature (Nakahara *et al.*, 2018), a meta-analysis of predominantly FreeSurfer 5.3 studies (Haukvik *et al.*, 2018) and studies that employed FreeSurfer 6.0 (Baglivo *et al.*, 2017; Ho *et al.*, 2017a, 2017b), we hypothesized a significant group by region interaction with the largest schizophrenia-control effect sizes for the DG/CA4 and CA1 and smallest effect sizes for the subicular regions. We also explored relationships between regions with the largest group difference effect sizes and cognitive

performance. To identify possible novel contributing genetic variants to schizophrenia-related HF subregion volume deficits, we performed, to our knowledge the first, schizophrenia genome-wide association (GWA) analysis with DG volume (largest group difference effect size) as the quantitative phenotype. Finally, we explored possible relationships between DG volume and age at onset, duration of illness, symptom severity, smoking, and medication dose.

Methods

Participants

Individuals with schizophrenia ($n = 176$, mean age ± s.d. = 38.9 ± 11.5, 132 males) and healthy volunteers ($n = 173$, mean age ± s.d. = 37.6 ± 11.3, 123 males) with similar mean age, gender handedness, and ethnicity distributions, recruited from seven sites, participated in this multi-center cross sectional case–control study (Table 1) (Friedman and Glover, 2006; Friedman *et al.*, 2006; Greve *et al.*, 2011; Glover *et al.*, 2012). Each participant was assessed with high-resolution T1-weighted scans and clinical assessments (Oldfield, 1971; de Belmont Hollingshead, 1975; Kay *et al.*, 1989; Uttl, 2002). Inclusion criteria were clinically stable – no antipsychotic medication or dose changes within the last two months – schizophrenia diagnosis based on DSM-IV-TR (First, 2002). Schizophrenia and healthy volunteers with a history of major medical illness, drug dependence in the last five years (except for nicotine), current substance abuse disorder, or MRI contraindications, were excluded. Excluded were individuals with schizophrenia with significant tardive dyskinesia and healthy volunteers with a current or past history of major neurological or psychiatric illness or a first-degree relative with an Axis-I psychotic disorder diagnosis (online Supplementary Methods). Written informed consent, including permission to share de-identified data between the centers, approved by the University of California (UC) Irvine, UC Los Angeles, and UC San Francisco, Duke University, University of North Carolina, New Mexico, Iowa, and Minnesota Institutional Review Boards, was obtained from all study participants.

Image analysis

Hippocampal tail, subiculum, CA1, hippocampal-fissure, presubiculum, parasubiculum, molecular layer of the hippocampus (molecular_layer_HP), granule cell and molecular cell layer of the DG (GC-ML-DG), CA3, CA4, fimbria, and hippocampal-amygdaloid transition region (HATA) (Fig. 1a) as well as intracranial volume (ICV) and overall hippocampal volumes (online Supplementary Table S1) were extracted from high-resolution T1-weighted images of the brain, that had previously been determined of good quality (little motion or other artifacts based on visual inspection) (van Erp *et al.*, 2014; Esteban *et al.*, 2017), using FreeSurfer 6.0 (https://surfer.nmr.mgh.harvard.edu) (Fischl *et al.*, 2002; Van Leemput *et al.*, 2008, 2009; Fischl, 2012; Iglesias *et al.*, 2013).

Neuropsychological battery

Study participants performed the Computerized Multiphasic Interactive Neurocognitive DualDisplay System (CMINDS®) FBIRN task battery and the attention/vigilance, speed of processing, working memory, verbal learning, visual learning, and reasoning/problem cognitive domain scores as well as a total composite (global cognition) score (online Supplementary

Table 1. Sample demographics and clinical characteristics

	Schizophrenia (n = 176)	Healthy volunteer (n = 173)	Statistic	p-value
Mean age (s.d.)	38.9 (11.5)	37.6 (11.3)	$t_{346} = 1.11$	0.27
Gender (M/F)	132/44	123/50	$\chi^2_1 = 0.36$	0.39
Handedness[a] (bilateral/left/right)	4/12/159	2/7/164	FET	0.40
Subject socioeconomic status[b] (s.d.)	4.6 (0.9)	5.7 (0.9)	$t_{347} = -11.18$	<0.0001
Parental socioeconomic status[b] (s.d.)	5.6 (1.7)	5.9 (1.5)	$t_{347} = -1.25$	0.21
NAART	29.6 (12.3)	39.8 (11.5)	$t_{343} = -7.92$	<0.0001
Ethnicity			FET	0.14
American Indian or Alaskan Native	3	3		
Asian	22	15		
Black or African American	35	19		
Native Hawaiian or Pacific Islander	2	2		
White	113	134		
Smoking status			$\chi^2_2 = 66.9$	<0.0001
Current smoker	79 (45%)	14 (8%)		
Ex-smoker	33 (19%)	32 (19%)		
Never-smoker	63 (36%)	127 (73%)		
Smoking – current pack-years	6.9 (13.1)	1.9 (7.1)	$t_{345} = 4.44$	<0.0001
Smoking – lifetime pack-years	10.7 (16.3)	2.3 (8.6)	$t_{344} = 6.02$	<0.0001
Age at onset	21.9 (7.8)			
Duration of illness	17.1 (11.6)			
PANSS positive	15.4 (5.2)			
PANSS negative	14.3 (5.4)			
PANSS general	28.2 (7.4)			
PANSS composite	1.1 (6.3)			

FET, Fisher's exact test; NAART, North American Adult Reading Test; PANSS, Positive and Negative Syndrome Scale.
[a]Based on Edinburgh Handedness Inventory.
[b]Based on the Education Level of the Hollingstead Socioeconomic Status Scale.

Table S2) were computed as described in detail previously (van Erp *et al.*, 2015).

Genetic imputation and quality control

DNA samples from unrelated and mixed ethnicity subjects (schizophrenia = 130, healthy volunteers = 145; online Supplementary Methods & Table S3) were genotyped using the Illumina MEGA + Psych chip (Illumina, SD, USA) between January 2016–May 2016 at Illumina Genomics Services (San Diego). Data were filtered to remove single-nucleotide polymorphisms (SNPs) with low minor allele frequency (MAF < 0.01), deviations from Hardy–Weinberg equilibrium ($p < 1 \times 10^{-6}$), or poor genotyping call rate (<95%) using PLINK software (http://pngu.mgh.harvard.edu/purcell/plink) (Purcell *et al.*, 2007). Filtered data were imputed to the 1000 Genomes Project reference panel (phase 1, version 3; ftp://ftp.1000genomes.ebi.ac.uk/vol1/ftp/release/20130502) using the Michigan imputation server (https://imputationserver.sph.umich.edu/index.html) (Das *et al.*, 2016).

For individuals with genotyping (n = 275; schizophrenia = 130, healthy volunteers = 145), imputed SNPs with estimated linkage

disequilibrium $R^2 < 0.8$ or low MAF (<0.5%) were removed, resulting in a final dataset of 12 049 533 SNPs.

Statistical analyses

Prior to the main multivariate statistical analyses, we ran univariate mixed-model regression analyses predicting ICV, left and right total hippocampal volumes (online Supplementary Results), and left and right HF subregions with group, site, gender, age, hemisphere (repeated measure), group × site, group × hemisphere, site × hemisphere, and group × site × hemisphere interactions to visually examine the residuals for normality (Proc Univariate, SAS v9.4, SAS Institute Inc.); analysis of ICV did not include a hemisphere term. Residuals appeared normally distributed, no additional data points were excluded, and no data transforms were applied.

To enable proper testing of the diagnosis × region interaction on on hippocampal subregion volumes, data were equated for scalar differences between the subregions by normalization to the mean healthy volunteers subregion volumes [normalized volume = (participant volume − healthy volunteer mean volume)/healthy
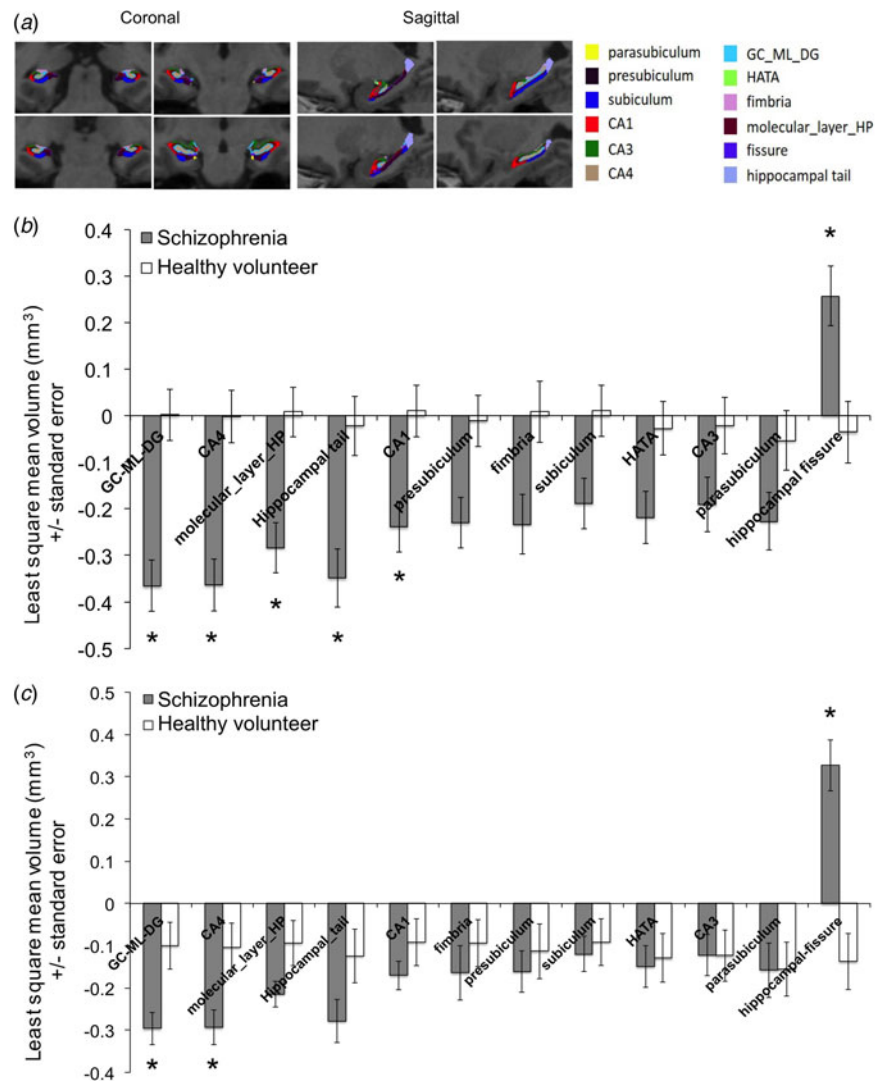
Fig. 1. Hippocampal formation subregion segmentations and least square mean normalized volumes. (a) Left shows hippocampal formation segmentations on 4 coronal slices from anterior (top) to posterior (bottom). Right row shows hippocampal formation segmentations on 4 left hemisphere sagittal slices from medial (top) to lateral (bottom). (b) Least square mean normalized hippocampal subregion volumes ± standard error by diagnosis (Model 1). The hippocampal subregion volumes are normalized to the control mean of left and right hemisphere subregion volumes, and statistical analyses controlled for ICV. (c) Least square mean normalized hippocampal subregion volumes ± standard errors by diagnosis (Model 2). The hippocampal subregion volumes are normalized to the control mean of left and right hemisphere subregion volumes, and statistical analyses controlled for left and right hippocampus volume. Schizophrenia (gray bars). Healthy volunteers (white bars). *Significant Bonferroni corrected group contrasts ($p < 0.004$).

volunteers standard deviation]. The normalization was performed with the healthy volunteer mean of left and right hemisphere volumes [mean across healthy volunteer subjects of (left + right volumes/2)] to allow for examination of hemisphere effects. The diagnosis × region interaction on hippocampal subregion volumes was also tested in a model excluding fissure volumes which should be larger in individuals with lower hippocampal volumes such as individuals with schizophrenia.

Group differences for each region were examined using mixed-model regression analyses (Proc Mixed, SAS v9.4, SAS Institute Inc.), predicting normalized hippocampal subregion volumes with group, region, and hemisphere and their two- and three-way interactions. Region and hemisphere entered the model as repeated measures factors, and gender, and site along with two- and three-way interactions between site, group, and region entered the model as categorical and age and ICV as continuous covariates (*Model 1*). Degrees of freedom were estimated using the Satterthwaite option. Possible confounding influences of smoking status on HF subregion volumes (Durazzo *et al.*, 2013; Schneider *et al.*, 2014) were assessed by including smoking status (current smoker, ex-smoker, never-smoker), current pack-year, or lifetime pack-year as covariates in *Model 1*, respectively. We also ran models in current non-smokers and never smokers only. Possible

confounding effects of ethnicity were examined and ethnicity was not found to be a significant predictor of HF subregion volumes ($p > 0.05$).

To assess the independence of the pattern of hippocampal subregion abnormalities from overall hippocampal volume deficits, a second analysis included *left and right hippocampal volumes*, instead of ICV, as covariates (*Model 2*). For the regions with *a priori* defined directional hypotheses based on the literature (CA1, CA2-3, DG/CA4, and subiculum) the significance threshold was set at $p < 0.05$ (one-tailed). We also indicate which of the findings pass the more conservative Bonferroni multiple comparison corrected threshold for a test of subregion differences of $p < 0.004$ ($0.05 \div 12$ hippocampal subregions, two tailed). Percent volume differences and Cohen's *d* weighted mean effect sizes, based on Model 1, were computed for each of the subregions.

We assessed the relationships between HF subregion volumes (with moderate between group effect sizes $d < -0.40$) and cognitive performance, age at onset, duration of illness, symptom severity (SANS and SAPS scores), and medication dose using regressions statistically controlling for sex, site (categorical), age, and ICV (two-tailed; online Supplementary Methods). Unequal slope analyses (comparing diagnoses) did not show significant

diagnosis × volume interactions on cognitive performance. Therefore, only overall sample associations with cognitive performance are reported and type I error was controlled using Bonferroni correction (see online Supplementary Table S2). All analyses only included subjects with available anatomical, cognitive, or symptom data, no extrapolation or imputation of these data was performed to generate missing data.

Genome-wide association and gene-based analyses

The GWA analysis predicted mean bilateral DG volume with diagnosis, SNP, and the diagnosis × SNP interaction, while statistically controlling for age, sex, whole hippocampus volume, site (scanner), and four multidimensional-scaling (MDS) components using PLINK. Whole hippocampal volume, rather than ICV was included in the GWA analysis, as it may more likely yield GWA findings unique to the DG volume. The standard genome-wide significant threshold of $p < 5 \times 10^{-8}$ was applied to identify significant SNP (Risch and Merikangas, 1996; Barsh *et al.*, 2012) and diagnosis × SNP interaction effects (Hancock *et al.*, 2012). A fast and flexible gene- or set-based association test using genome-wide association study (GWAS) summary data of DG volume was performed using GCTA (see online Supplementary Methods). The Manhattan plot (Fig. 2) was created using SNP2GENE software (http://fuma.ctglab.nl/) (Watanabe *et al.*, 2017). Genome-wide significance of gene was defined at $p = 0.05/24\,765$ (the number of total genes) $= 2.0 \times 10^{-6}$.

Results

Main and interaction effects on HF subregion volumes

Mixed-model regression analyses, controlling for individual differences in ICV (Model 1), showed significant main effects of diagnosis, region, hemisphere, gender, site, and ICV as well as significant diagnosis × region, hemisphere × region, diagnosis × site, and site × region interactions on HF subregion volumes (Table 2). Mixed-model regression analyses, controlling for individual differences in left and right hippocampal volume (Model 2), showed significant main effects of region, hemisphere, gender, age, site, and hippocampal volume, as well as significant diagnosis × region, hemisphere × region, and site × region interactions, though the effects of diagnosis was no longer significant (Table 2). The diagnosis × region interaction was also significant when fissure volumes were excluded from the analysis [$F_{(10,613)} = 2.64$, $p < 0.004$ (Model 1); $F_{(10,635)} = 2.83$, $p < 0.002$ (Model 2)].

Decomposition of the diagnosis × region interaction in the model controlling for ICV (Model 1) showed that subjects with schizophrenia, compared to healthy subjects, had significantly smaller GC-ML-DG ($t_{644} = -4.82$, $p < 0.0001$; -4.1%, Cohen's $d = -0.57$), CA4 ($t_{640} = -4.64$, $p \leqslant 0.001$; -4.0%, $d = -0.55$), molecular_layer_HP ($t_{644} = -3.94$, $p \leqslant 0.0001$; -4.0%, $d = -0.47$), hippocampal tail ($t_{660} = -3.7$, $p = 0.0002$; -3.1%, $d = -0.44$), CA1 ($t_{645} = -3.26$, $p = 0.001$; -3.1%, $d = -0.39$), presubiculum ($t_{645} = -2.88$, $p = 0.004$; -2.9%, $d = -0.34$), fimbria ($t_{623} = -3.67$, $p = 0.008$; -5.4%, $d = -0.32$), subiculum ($t_{650} = -2.61$, $p = 0.009$; -2.3%, $d = -0.31$), HATA ($t_{641} = -2.41$, $p = 0.02$; -3.0%, $d = -0.29$), CA3 ($t_{635} = -2.03$, $p < 0.04$; -2.4%, $d = -0.24$), and parasubiculum ($t_{615} = -1.97$, $p < 0.05$; -3.4%, $d = -0.24$) volumes, and larger hippocampal fissure ($t_{632} = 3.18$, $p = 0.002$; $+5.0\%$, $d = 0.38$) volumes (all p-value reported are two-tailed). GC-ML-DG, CA4, molecular_layer_HP, hippocampal tail,

CA1, and hippocampal fissure group differences were also significant at the Bonferroni multiple comparison correction threshold of $p < 0.004$ when controlling for ICV (Fig. 1b).

Decomposition of the diagnosis × region interaction in the model controlling for hippocampal volume (Model 2) showed a similar profile to that in model 1. Subjects with schizophrenia, compared to healthy subjects, had significantly smaller GC-ML-DG ($t_{599} = -3.6$, $p = 0.0003$; Cohen's $d = -0.43$), CA4 ($t_{605} = -3.25$, $p = 0.001$; $d = -0.39$), molecular_layer_HP ($t_{490} = -2.8$, $p = 0.005$; $d = -0.33$), and hippocampal tail ($t_{645} = -2.14$, $p < 0.03$; $d = -0.26$), but not CA1 ($d = -0.20$), presubiculum ($d = -0.09$), fimbria ($d = -0.08$), subiculum ($d = -0.06$), HATA ($d = -0.03$), CA3 ($d = 0$), and parasubiculum ($d = 0$); in this secondary analysis, the hippocampal fissure remained significantly larger in schizophrenia compared with healthy volunteers ($t_{638} = 5.36$, $p < 0.0001$; $d = 0.65$) volumes. Only the GC-ML-DG, CA4, molecular_layer_HP, and hippocampal fissure group differences were significant at the Bonferroni multiple comparison correction threshold of $p < 0.004$ when controlling for hippocampal volume (Fig. 1c). Given that DG volume showed the largest differences between individuals with schizophrenia and healthy volunteers, further association and GWA analysis focused on this region.

Decomposition of the region × hemisphere interaction based on the Model 1 analysis showed that left hemisphere GC-ML-DG, CA1, CA3, CA4, molecular_layer_HP, hippocampal tail, and HATA region volumes were smaller than right hemisphere volumes (all p-values <0.0001), while left hemisphere subiculum ($p < 0.05$), presubiculum ($p < 0.0001$), and parasubiculum volumes were larger than right hemisphere volumes. Left and right hemisphere volumes for the fimbria and hippocampal fissure were equivalent. Finally, there is a consistent pattern of lower GC-ML-DG volume in individuals with schizophrenia compared with controls across the seven sites (online Supplementary Fig. S2).

Associations with neuropsychological performance

DG (GC-ML-DG) and CA4 volumes showed significant associations with visual learning and speed of processing, molecular layer volumes showed significant associations with visual learning and CMINDS composite, while the hippocampal tail showed significant associations with attention/vigilance ($p < 0.0018$, $0.05/7/4 = 0.0018$, Bonferroni; see online Supplementary Table S2).

Novel genome-wide markers associated with DG volume

No SNPs showed a genome-wide significant main effect on DG volume. The GWA analysis did identify a genome-wide significant diagnosis × SNP interaction ($p < 5 \times 10^{-8}$) on DG volume for rs56055643 ($\beta = 10.75$, 95% CI 7.0–14.5; S.E. = 1.91; T-statistic = 5.63, $p = 4.8 \times 10^{-8}$) located on Chromosome 3 near *MOBP* (Fig. 2 and online Supplementary Table S4). Decomposition of the diagnosis × SNP interaction showed a positive main effect of the rs56055643 A allele in schizophrenia ($\beta = 4.79$, 95% CI 1.8–7.82; S.E. = 1.54; T-statistic = 3.10, $p = 0.002$) and a negative main effect of the rs56055643 A allele in healthy volunteers ($\beta = -5.14$, 95% CI -7.9 to 2.41; S.E. = 1.40; T-statistic = -3.69, $p = 0.0003$; Fig. 2d). The effect of genotype remained significant within the schizophrenia group when either antipsychotic type (typical, atypical, both, or none) or chlorpromazine medication dose were included as covariates in the analysis. Gene-based analysis based on this GWA summary found that several
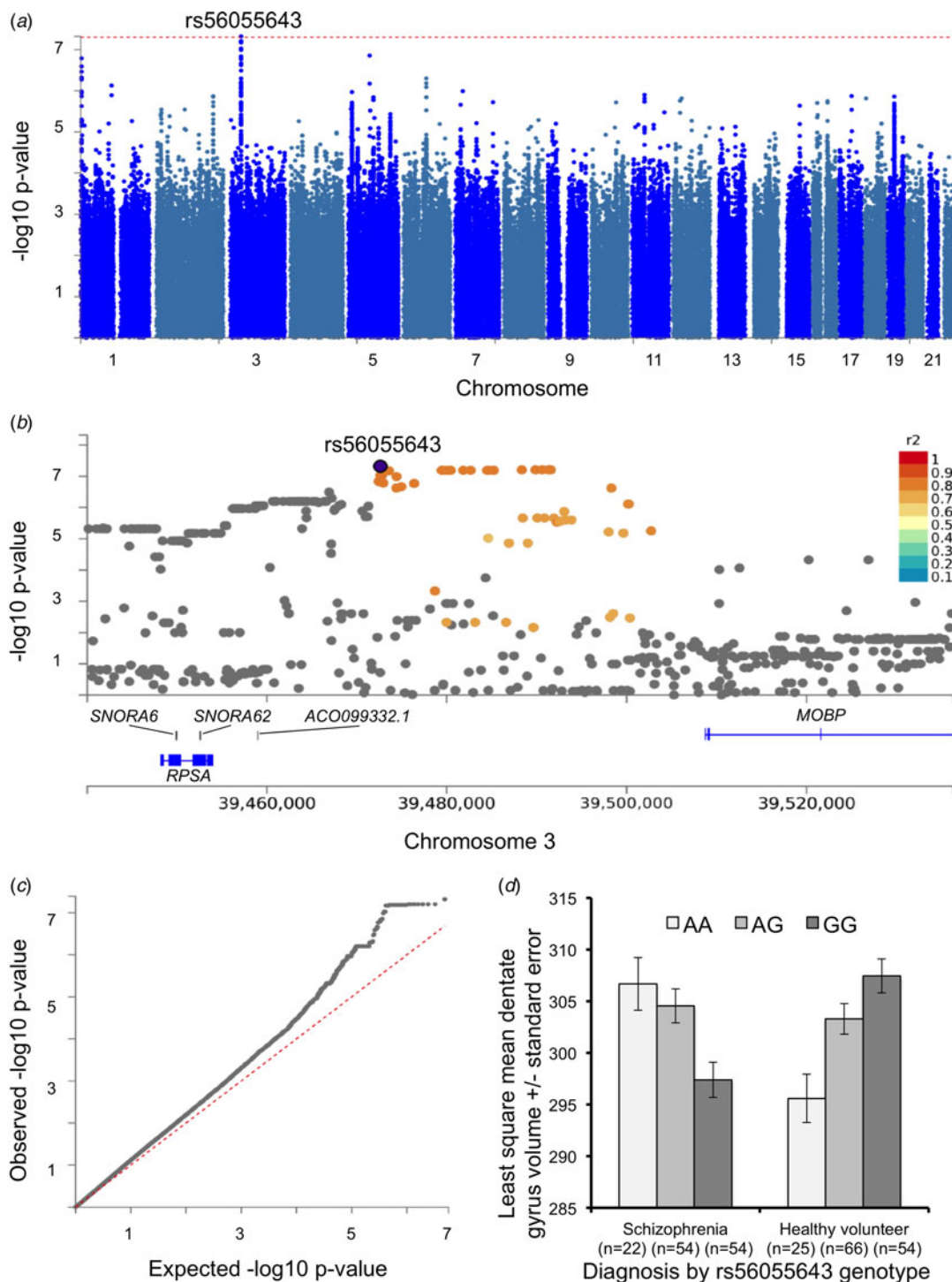
Fig. 2. Genome-wide association with dentate gyrus volume. (a) A Manhattan plot displays the association *p* value for each SNP in the genome (displayed as −log10 of the *p*-value). Red line displays $p = 5 \times 10^{-8}$ line. (b) Detailed Manhattan plot around top SNP (rs56055643) along with gene mapping. SNPs in genomic risk loci are color-coded as a function of their maximum r^2 to one of the independent significant SNPs in the locus, as follows: red ($r^2 > 0.8$), orange ($r^2 > 0.6$), green ($r^2 > 0.4$), blue ($r^2 > 0.2$), and gray ($r^2 \leqslant 0.2$). (c) Quantile–quantile plot for GWAS results. The empirical and theoretical distributions are shown as black and red lines, respectively. (d) Depiction of the diagnosis by rs56055643 interaction on dentate gyrus volume (±standard error).

additional genes, including *MOBP*, *RPSA*, and *SLC25A38*, were significantly associated with DG volume (Table 3). The gene expression heatmap shows that each of these genes is expressed in the brain, including in the hippocampus (online Supplementary Fig. S1).

Discussion

We found, to our knowledge for the first time, a significant group by HF subregion interaction, indicating regional variation in HF volume deficits in schizophrenia, significant associations between

Table 2. Effects on hippocampal subregion volumes based on multivariate mixed-model regression analyses

Effect	Model 1				Model 2			
	nDF	dDF	F-value	p-value	nDF	dDF	F-value	p-value
Diagnosis	1	636	18.19	**<0.0001**	1	634	1.95	0.16
Region	11	618	3.39	**0.0001**	11	622	3.47	**0.0001**
Diagnosis × region	11	618	4.06	**<0.0001**	11	622	4.15	**<0.0001**
Hemisphere	1	507	30.76	**<0.0001**	1	637	11.71	**0.0007**
Diagnosis × hemisphere	1	507	1.19	0.28	1	615	1.31	0.25
Hemisphere × region	11	629	32.19	**<0.0001**	11	627	31.30	**<0.0001**
Diagnosis × hemisphere × region	11	629	1.82	0.05	11	627	1.77	0.06
Site	6	637	15.39	**<0.0001**	6	631	1.50	0.18
Diagnosis × site	6	631	2.18	**0.04**	6	625	0.89	0.50
Site × region	66	618	2.54	**<0.0001**	66	622	2.61	**<0.0001**
Diagnosis × site × region	66	618	1.11	0.26	66	622	1.14	0.21
Sex	1	652	11.84	**0.0006**	1	632	39.26	**<0.0001**
Age	1	652	0.10	0.75	1	628	26.30	**<0.0001**
ICV	1	652	293.09	**<0.0001**				
Hippocampus volume					1	657	3504.73	**<0.0001**

nDF, nominator degrees of freedom; dDF, denominator degrees of freedom.
Model 1 statistically controls for individual differences in intracranial volume (ICV). Model 2 statistically controls for individual differences in hippocampal volume.
p-values <0.05 are listed in bold.

Table 3. Gene-based analysis based on dentate gyrus genome-wide association results

Gene	CHR	Start	End	Gene based p-value
SLC25A38	3	39 424 839	39 438 842	9.59×10^{-8}
RPSA	3	39 448 180	39 454 033	8.88×10^{-8}
MOBP	3	39 508 689	39 570 970	3.27×10^{-5}

CHR: chromosome; Start: start location of gene in base pairs; End: end location of gene in base pairs; Gene based p-value: gene-based test p-value based on GCTA. The association p-value for a set of SNPs (±50 Kb of UTRs) from an approximated distribution of the sum of χ^2-statistics over the SNPs was calculated based on the GWAS data and LD correlations between SNPs from 1000 Genomes Project samples as a reference. Genome-wide significance was defined at p = 0.05/24 765 (the number of total genes) = 0.0000020

DG volumes and visual memory and speed of processing in the overall sample, and a genome-wide significant SNP associated with DG volume.

All HF subregion volumes were smaller and hippocampal fissure volume was larger (at $p < 0.05$) in individuals with schizophrenia compared to healthy controls when controlling for individual differences in ICV; GC-ML-DG, CA4, molecular_layer_HP, hippocampal tail, CA1, and hippocampal fissure volume group differences survived multiple comparison correction.

GC-ML-DG, CA4, molecular_layer_HP, and hippocampal tail volumes were smaller and hippocampal fissure volume was larger (at $p < 0.05$) in individuals with schizophrenia compared to healthy controls when controlling for individual differences in hippocampal volumes; GC-ML-DG, CA4, and hippocampal fissure group differences survived multiple comparison correction.

We found that these regional volume abnormalities were independent of possible confounding effects of differences in smoking habits between schizophrenia and healthy volunteers, were not associated with ethnicity, and were not correlated with antipsychotic medication dose.

Our findings are largely consistent with prior studies that also found CA1, CA2/3, CA4/DG, molecular_layer_HP, subiculum, presubiculum, hippocampal tail volume deficits (Francis et al., 2013; Mathew et al., 2014; Haukvik et al., 2015; Kawano et al., 2015; Hýža et al., 2016; Ho et al., 2017a, 2017b; Ota et al., 2017; Rhindress et al., 2017) at $p < 0.05$. Moreover, our FreeSurfer 6.0 findings are also consistent with a recent meta-analysis, which reported the largest effect size for combined DG/CA4 volume deficits in schizophrenia based on predominantly FreeSurfer 5.3 studies (Haukvik et al., 2018). Lower bilateral CA4, DG, and CA1 volumes have also been observed in individuals with first-episode psychosis (Baglivo et al., 2017). We found fimbria ($p < 0.05$) and fissure volume abnormalities in schizophrenia compared to healthy volunteers, which were not reported previously. Possible reasons for the discrepancy are lower measurement accuracy of the smaller subregions, as well as between study differences in status and duration of illness (Ho et al., 2017a). FreeSurfer 6.0 enables separate estimates for GC-ML-DG, CA4, and CA3 volumes, which was not possible in previous FreeSurfer versions (5.1/5.3). Our finding that DG volume is significantly smaller in schizophrenia compared to control subjects based on FreeSurfer 6.0, corroborates that from an independent study that assessed HF volumes with automatic segmentation of hippocampal subfields (ASHS) (Ota et al., 2017).

Furthermore, while some studies suggest that hippocampal volume deficits are largely similar across subregions (Haukvik et al., 2015), the present study found a significant group × region interaction even when controlling for whole hippocampal volume. These findings indicate regional variability in HF subregion volume abnormalities in schizophrenia independent from overall

hippocampal volume. Moreover, the interaction remained significant when the hippocampal fissure was excluded from the analysis. The present study thus provides robust evidence for regional variability in volume deficits within the HF in schizophrenia.

DG volume was significantly positively associated with visual memory and speed of processing performance in the overall sample, findings that are in line with the dysfunctional DG hypothesis in schizophrenia (Tamminga *et al.*, 2010, 2012). Interestingly, several mouse models of schizophrenia – including Ca^{2+}/calmodulin-dependent protein kinase IIα heterozygous, Schnurri-2 knockout, mutant synaptosomal-associated protein 25 knock-in, and forebrain-specific calcineurin knockout mice – show DG dysfunction due to an immature DG, which has also been observed in schizophrenia (Walton *et al.*, 2012) and could underlie the observed volume deficit (Hagihara *et al.*, 2013; Ohira *et al.*, 2013). These mouse models of psychosis all show memory deficits, suggesting that DG dysfunction may be associated with memory deficits in schizophrenia. Though, the association between visual memory and volume was not unique to the DG, and was also observed for the CA4 and the molecular layer. Differential associations between HF subregion volumes and cognitive performance will require additional study and replication. We found no significant associations between DG volume and age at onset, duration of illness, or symptom severity, though associations between brain volumes and symptom measures are often weak and may require larger samples.

Although there have been several GWA studies on hippocampal volume, to our knowledge this is the first report to identify loci associated with DG volume in a schizophrenia sample. The top SNP, rs56055643, with a *p*-value less than the 5×10^{-8} standard genome-wide threshold, and several SNPs in high linkage disequilibrium with *p*-values less than 1×10^{-7} are located on chromosome 3 near the genes *RPSA* and *MOBP*. The gene-based analysis also suggests the association of these genes with DG volume.

RPSA, expressed in the hippocampus, encodes 40S ribosomal protein SA that is required for the assembly and/or stability of the 40S ribosomal subunit. This protein plays a role as a cell surface receptor for laminin, which plays an important role in cell differentiation, migration, and adhesion as well as synapse stabilization (Omar *et al.*, 2017). Importantly, this protein interacts with ZNF804A, a well-known schizophrenia risk gene (Steinberg *et al.*, 2011; Zhang *et al.*, 2011), and rescues the migration and translational defects caused by *ZNF804A* knockdown. RPSA is enriched in mature compared to immature DG granule cells (Chatzi *et al.*, 2016) consistent with models that have hypothesized an immature DG in schizophrenia (Walton *et al.*, 2012).

MOBP, expressed in hippocampal oligodendrocytes, encodes myelin-associated oligodendrocyte basic protein. Recent studies suggest that oligodendrocyte function and myelination are disrupted in schizophrenia (Kubicki *et al.*, 2005; McInnes and Lauriat, 2006) and a study combining PGC schizophrenia risk loci, lifespan gene expression data, and schizophrenia methylome data has identified *MOBP* as an SNP-rich gene expression hub (Hegyi, 2017). Lower numbers of oligodendrocytes have been observed in the hippocampal CA4 subfield in individuals with schizophrenia (Schmitt *et al.*, 2009) and altered levels of myelin basic protein (MBP) have been reported in schizophrenia and bipolar disorder compared to controls (Chambers and Perrone-Bizzozero, 2004) providing evidence for the myelin hypothesis in schizophrenia. Muted myelination could contribute to lower

CA4 and DG volumes in schizophrenia. The rs56055643 SNP, located on near *MOBP*, was also associated with CA4 volume ($\beta = 9.30$, 95% CI 5.77–12.82, S.E. = 1.80; *T*-statistic = 5.17, $p = 4.7 \times 10^{-7}$) but not with whole hippocampus volume ($p = 0.64$). Likewise, the gene-based analysis also showed that *MOBP* is associated with CA4 ($p = 0.0002$) but not with whole hippocampus volume ($p = 0.60$).

SLC25A38, or appoptosin, belongs to the SCL25 mitochondria solute carrier family, is expressed in hippocampal neurons, and has been linked to apoptosis (Zhang *et al.*, 2012). Moreover, *MOBP* SNPs were strongly associated with appoptosin expression (Höglinger *et al.*, 2011). These findings may suggest that *SLC25A39* and *MOBP* may be differentially involved in the regulation of survival or maturation of newly generated DG neurons in schizophrenia compared to controls (Chambers and Perrone-Bizzozero, 2004).

It has been argued that imaging associations that are observed only in patients should be viewed with caution (Carter *et al.*, 2017). We agree with this viewpoint but also note that genetic loci may have differential effects within the context of a disease. Therefore testing for diagnosis by SNP interaction effects may provide additional insights that may be missed when testing only for main effects of SNPs across diagnostic groups. Moreover, the observation that rs56055643 alleles show opposing effects in individuals with schizophrenia and healthy individuals could not have been observed in studies that perform genetic analyses using categorical (e.g. case–control) as opposed to quantitative traits.

This imaging study has several notable strengths. First, this study has a robust sample size for an imaging study including 176 schizophrenia and 173 healthy subjects recruited from multiple centers strengthening the generalizability of the findings. Second, this study demonstrated a significant group × region interaction on hippocampal subregion volumes indicating, to our knowledge for the first time, that in schizophrenia, not all HF subregions are affected equally. Third, the percent difference in volume between schizophrenia and healthy volunteers tracks the group contrast effect sizes and suggest that the effect sizes are not merely due to differences in measurement error between the regions. Fourth, this study tests for group by SNP interactions on a quantitative phenotype, an analysis strategy that is less frequently employed but may yield novel insights into gene–phenotype relationships. Finally, this study adheres to the best of its abilities to the 'Strengthening the Reporting of Observational Studies in Epidemiology (STROBE) and Strengthening the REporting of Genetic Association studies' (STREGA) guidelines (online Supplementary Table S5).

Some limitations must also be noted. First, FreeSurfer's hippocampal subregion method was developed using ultra-high-resolution brain imaging data with a within-plane resolution of 380 μm and 0.8 mm slice thickness (Van Leemput *et al.*, 2008) and may require additional validation for use with conventional resolution imaging data. It should be noted that our findings in part replicate previous reports based on ultra-high-resolution scans as discussed above (Ota *et al.*, 2017), corroborating prior reports that the method may also be applicable to high-quality conventional resolution structural imaging data (Iglesias *et al.*, 2013). Furthermore, the fact that most subregion volumes are smaller while the fissure is larger in individuals with schizophrenia when compared to healthy controls indicates that the method makes local adjustments to the subregions. Second, we report to our knowledge a first GWAS with DG volume as a quantitative trait in schizophrenia and these findings warrant replication

in an independent sample. Third, while no effects of ethnicity on HF subregion volumes were observed and while differences in ethnicity in the GWA analyses were controlled for using MDS components, only analyses in ethnically homogeneous samples can fully exclude ethnic influences on GWA findings. Finally, while the use of multi-scanner imaging data may be viewed as a weakness, numerous studies have shown that larger samples based on multi-scanner data improves power to detect effects rather than increases noise over signal (Fennema-Notestine *et al.*, 2007; Segall *et al.*, 2009; van Erp *et al.*, 2014; Boedhoe *et al.*, 2017). Moreover, mean DG volume was smaller in schizophrenia than healthy subjects within each site.

In conclusion, we found volumetric abnormalities in some but not all hippocampal subregions in schizophrenia. In particular, DG was most severely affected and associated with visual memory and speed of processing deficits. Further, we identified novel genome-wide significant loci associated with DG volume. These findings support the DG dysfunction hypothesis of psychosis in schizophrenia (Tamminga *et al.*, 2010, 2012). They also suggest novel biological insights in DG pathophysiology [e.g. oligo-dendrocyte (*MOBP*), cell differentiation, migration, adhesion (*RPSA*), or maturation/apoptosis (*SLC25A38*) aberrancies]. Overall, our finding that not all HF subregion volumes are equally affected in schizophrenia suggests the involvement of different biological mechanisms between HF subregion, and that examining HF subregion abnormalities, including DG morphology and function as representative intermediate phenotypes, combined with genetics may allow for more accurate identification of the role of the HF in schizophrenia.

References

Adler DH, Pluta J, Kadivar S, Craige C, Gee JC, Avants BB and Yushkevich PA (2014) Histology-derived volumetric annotation of the human hippocampal subfields in postmortem MRI. *NeuroImage* **84**, 505–523.

Amaral DG and Witter MP (1989) The three-dimensional organization of the hippocampal formation: a review of anatomical data. *Neuroscience* **31**, 571–591.

Amaral DG, Scharfman HE and Lavenex P (2007) The dentate gyrus: fundamental neuroanatomical organization (dentate gyrus for dummies). *Progress in Brain Research* **216**, 3–22.

Baglivo V, Cao B, Mwangi B, Bellani M, Perlini C, Lasalvia A, Dusi N, Bonetto C, Cristofalo D, Alessandrini F, Zoccatelli G, Ciceri E, Dario L, Enrico C, Francesca P, Mazzi F, Paolo S, Balestrieri M, Soares JC, Ruggeri M and Brambilla P, GET UP Group (2017) Hippocampal subfield volumes in patients with first-episode psychosis. *Schizophrenia Bulletin* **44**, 552–559.

Barsh GS, Copenhaver GP, Gibson G and Williams SM (2012) Guidelines for genome-wide association studies. *PLoS Genetics* **8**, e1002812.

Boedhoe PSW, Schmaal L, Abe Y, Ameis SH, Arnold PD, Batistuzzo MC, Benedetti F, Beucke JC, Bollettini I, Bose A, Brem S, Calvo A, Cheng Y, Cho KIK, Dallaspezia S, Denys D, Fitzgerald KD, Fouche J-P, Giménez M, Gruner P, Hanna GL, Hibar DP, Hoexter MQ, Hu H, Huyser C, Ikari K, Jahanshad N, Kathmann N, Kaufmann C, Koch K, Kwon JS, Lazaro L, Liu Y, Lochner C, Marsh R, Martínez-Zalacaín I, Mataix-Cols D, Menchón JM, Minuzzi L, Nakamae T, Nakao T, Narayanaswamy JC, Piras F, Piras F, Pittenger C, Reddy YCJ, Sato JR, Simpson HB, Soreni N, Soriano-Mas C, Spalletta G, Stevens MC, Szeszko PR, Tolin DF, Venkatasubramanian G, Walitza S, Wang Z, van Wingen GA, Xu J, Xu X, Yun J-Y, Zhao Q, ENIGMA OCD Working Group, Thompson PM, Stein DJ and van den Heuvel OA (2017) Distinct subcortical volume alterations in pediatric and adult OCD: a worldwide meta- and mega-analysis. *The American Journal of Psychiatry* **174**, 60–69.

Carter CS, Bearden CE, Bullmore ET, Geschwind DH, Glahn DC, Gur RE, Meyer-Lindenberg A and Weinberger DR (2017) Enhancing the informativeness and replicability of imaging genomics studies. *Biological Psychiatry* **82**, 157–164.

Chambers JS and Perrone-Bizzozero NI (2004) Altered myelination of the hippocampal formation in subjects with schizophrenia and bipolar disorder. *Neurochemical Research* **29**, 2293–2302.

Chatzi C, Zhang Y, Shen R, Westbrook GL and Goodman RH (2016) Transcriptional profiling of newly generated dentate granule cells using TU tagging reveals pattern shifts in gene expression during circuit integration. *eNeuro* **3**, 1–17.

Das S, Forer L, Schönherr S, Sidore C, Locke AE, Kwong A, Vrieze SI, Chew EY, Levy S, McGue M, Schlessinger D, Stambolian D, Loh P-R, Iacono WG, Swaroop A, Scott LJ, Cucca F, Kronenberg F, Boehnke M, Abecasis GR and Fuchsberger C (2016) Next-generation genotype imputation service and methods. *Nature Genetics* **48**, 1284–1287.

de Belmont Hollingshead A (1975) *Four Factor Index of Social Status*. Unpublished Working Paper, Yale University, New Haven, CT.

Durazzo TC, Pennington DL, Schmidt TP, Mon A, Abé C and Meyerhoff DJ (2013) Neurocognition in 1-month-abstinent treatment-seeking alcohol-dependent individuals: interactive effects of age and chronic cigarette smoking. *Alcoholism, Clinical and Experimental Research* **37**, 1794–1803.

Esteban O, Birman D, Schaer M, Koyejo OO, Poldrack RA and Gorgolewski KJ (2017) MRIQC: advancing the automatic prediction of image quality in MRI from unseen sites. *PLoS ONE* **12**, e0184661.

Fennema-Notestine C, Gamst AC, Quinn BT, Pacheco J, Jernigan TL, Thal L, Buckner R, Killiany R, Blacker D, Dale AM, Fischl B, Dickerson B and Gollub RL (2007) Feasibility of multi-site clinical structural neuroimaging studies of aging using legacy data. *Neuroinformatics* 5, 235–245.

First MB (2002) *User's Guide for the Structured Clinical Interview for DSM-IV-TR Axis I Disorders: SCID-I*. Washington DC: American Psychiatric Press, Inc.

Fischl B (2012) Freesurfer. *NeuroImage* 62, 774–781.

Fischl B, Salat DH, Busa E, Albert M, Dieterich M, Haselgrove C, van der Kouwe A, Killiany R, Kennedy D, Klaveness S, Montillo A, Makris N, Rosen B and Dale AM (2002) Whole brain segmentation: automated labeling of neuroanatomical structures in the human brain. *Neuron* 33, 341–355.

Francis AN, Seidman LJ, Tandon N, Shenton ME, Thermenos HW, Mesholam-Gately RI, van Elst LT, Tuschen-Caffier B, DeLisi LE and Keshavan MS (2013) Reduced subicular subdivisions of the hippocampal formation and verbal declarative memory impairments in young relatives at risk for schizophrenia. *Schizophrenia Research* 151, 154–157.

Friedman L and Glover GH (2006) Report on a multicenter fMRI quality assurance protocol. *Journal of Magnetic Resonance Imaging* 23, 827–839.

Friedman L, Glover GH and Fbirn Consortium (2006) Reducing interscanner variability of activation in a multicenter fMRI study: controlling for signal-to-fluctuation-noise-ratio (SFNR) differences. *NeuroImage* 33, 471–481.

Glover GH, Mueller BA, Turner JA, van Erp TGM, Liu TT, Greve DN, Voyvodic JT, Rasmussen J, Brown GG, Keator DB, Calhoun VD, Lee HJ, Ford JM, Mathalon DH, Diaz M, O'Leary DS, Gadde S, Preda A, Lim KO, Wible CG, Stern HS, Belger A, McCarthy G, Ozyurt B and Potkin SG (2012) Function biomedical informatics research network recommendations for prospective multicenter functional MRI studies. *Journal of Magnetic Resonance Imaging: JMRI* 36, 39–54.

Greenspan KS, Arakelian CR and van Erp TGM (2016) Heritability of hippocampal formation sub-region volumes. *Journal of Neurology and Neuroscience* 7, 1–7.

Greve DN, Mueller BA, Liu T, Turner JA, Voyvodic J, Yetter E, Diaz M, McCarthy G, Wallace S, Roach BJ, Ford JM, Mathalon DH, Calhoun VD, Wible CG, Brown GG, Potkin SG and Glover G (2011) A novel method for quantifying scanner instability in fMRI. *Magnetic Resonance in Medicine* 65, 1053–1061.

Hagihara H, Takao K, Walton NM, Matsumoto M and Miyakawa T (2013) Immature dentate gyrus: an endophenotype of neuropsychiatric disorders. *Neural Plasticity* 2013, 318596.

Haijma SV, Van Haren N, Cahn W, Koolschijn PCMP, Hulshoff Pol HE and Kahn RS (2013) Brain volumes in schizophrenia: a meta-analysis in over 18 000 subjects. *Schizophrenia Bulletin* 39, 1129–1138.

Hancock DB, Soler Artigas M, Gharib SA, Henry A, Manichaikul A, Ramasamy A, Loth DW, Imboden M, Koch B, McArdle WL, Smith AV, Smolonska J, Sood A, Tang W, Wilk JB, Zhai G, Zhao JH, Aschard H, Burkart KM, Curjuric I, Eijgelsheim M, Elliott P, Gu X, Harris TB, Janson C, Homuth G, Hysi PG, Liu JZ, Loehr LR, Lohman K, Loos RJF, Manning AK, Marciante KD, Obeidat M, Postma DS, Aldrich MC, Brusselle GG, Chen T-H, Eiriksdottir G, Franceschini N, Heinrich J, Rotter JI, Wijmenga C, Williams OD, Bentley AR, Hofman A, Laurie CC, Lumley T, Morrison AC, Joubert BR, Rivadeneira F, Couper DJ, Kritchevsky SB, Liu Y, Wjst M, Wain LV, Vonk JM, Uitterlinden AG, Rochat T, Rich SS, Psaty BM, O'Connor GT, North KE, Mirel DB, Meibohm B, Launer LJ, Khaw K-T, Hartikainen A-L, Hammond CJ, Gläser S, Marchini J, Kraft P, Wareham NJ, Völzke H, Stricker BHC, Spector TD, Probst-Hensch NM, Jarvis D, Jarvelin M-R, Heckbert SR, Gudnason V, Boezen HM, Barr RG, Cassano PA, Strachan DP, Fornage M, Hall IP, Dupuis J, Tobin MD and London SJ (2012) Genome-wide joint meta-analysis of SNP and SNP-by-smoking interaction identifies novel loci for pulmonary function. *PLoS Genetics* 8, e1003098.

Haukvik UK, Westlye LT, Mørch-Johnsen L, Jørgensen KN, Lange EH, Dale AM, Melle I, Andreassen OA and Agartz I (2015) In vivo hippocampal subfield volumes in schizophrenia and bipolar disorder. *Biological Psychiatry* 77, 581–588.

Haukvik UK, Tamnes CK, Söderman E and Agartz I (2018) Neuroimaging hippocampal subfields in schizophrenia and bipolar disorder: a systematic review and meta-analysis. *Journal of Psychiatric Research* 104, 217–226.

Hegyi H (2017) Connecting myelin-related and synaptic dysfunction in schizophrenia with SNP-rich gene expression hubs. *Scientific Reports* 7, 45494.

Ho NF, Holt DJ, Cheung M, Iglesias JE, Goh A, Wang M, Lim JK, de Souza J, Poh JS, See YM, Adcock AR, Wood SJ, Chee MW, Lee J and Zhou J (2017a) Progressive decline in hippocampal CA1 volume in individuals at ultra-high-risk for psychosis who do not remit: findings from the longitudinal youth at risk study. *Neuropsychopharmacology* 42, 1361–1370.

Ho NF, Iglesias JE, Sum MY, Kuswanto CN, Sitoh YY, De Souza J, Hong Z, Fischl B, Roffman JL, Zhou J, Sim K and Holt DJ (2017b) Progression from selective to general involvement of hippocampal subfields in schizophrenia. *Molecular Psychiatry* 22, 142–152.

Höglinger GU, Melhem NM, Dickson DW, Sleiman PMA, Wang L-S, Klei L, Rademakers R, de Silva R, Litvan I, Riley DE, van Swieten JC, Heutink P, Wszolek ZK, Uitti RJ, Vandrovcova J, Hurtig HI, Gross RG, Maetzler W, Goldwurm S, Tolosa E, Borroni B, Pastor P, PSP Genetics Study Group, Cantwell LB, Han MR, Dillman A, van der Brug MP, Gibbs JR, Cookson MR, Hernandez DG, Singleton AB, Farrer MJ, Yu C-E, Golbe LI, Revesz T, Hardy J, Lees AJ, Devlin B, Hakonarson H, Müller U and Schellenberg GD (2011) Identification of common variants influencing risk of the tauopathy progressive supranuclear palsy. *Nature Genetics* 43, 699–705.

Hýža M, Kuhn M, Češková E, Ustohal L and Kašpárek T (2016) Hippocampal volume in first-episode schizophrenia and longitudinal course of the illness. *The World Journal of Biological Psychiatry* 17, 429–438.

Iglesias JE, Sabuncu MR and Van Leemput K, Alzheimer's Disease Neuroimaging Initiative (2013) Improved inference in Bayesian segmentation using Monte Carlo sampling: application to hippocampal subfield volumetry. *Medical Image Analysis* 17, 766–778.

Kawano M, Sawada K, Shimodera S, Ogawa Y, Kariya S, Lang DJ, Inoue S and Honer WG (2015) Hippocampal subfield volumes in first episode and chronic schizophrenia. *PLoS ONE* 10, e0117785.

Kay SR, Opler LA and Lindenmayer J-P (1989) The positive and negative syndrome scale (PANSS): rationale and standardisation. *British Journal of Psychiatry* 155, 59–65.

Kubicki M, McCarley RW and Shenton ME (2005) Evidence for white matter abnormalities in schizophrenia. *Current Opinion in Psychiatry* 18, 121–134.

Mathew I, Gardin TM, Tandon N, Eack S, Francis AN, Seidman LJ, Clementz B, Pearlson GD, Sweeney JA, Tamminga CA and Keshavan MS (2014) Medial temporal lobe structures and hippocampal subfields in psychotic disorders: findings from the Bipolar-Schizophrenia Network on Intermediate Phenotypes (B-SNIP) study. *JAMA Psychiatry* 71, 769–777.

McInnes LA and Lauriat TL (2006) RNA metabolism and dysmyelination in schizophrenia. *Neuroscience and Biobehavioral Reviews* 30, 551–561.

Nakahara S, Matsumoto M and van Erp TGM (2018) Hippocampal subregion abnormalities in schizophrenia: a systematic review of structural and physiological imaging studies. *Neuropsychopharmacology Reports* 38, 156–166.

Ohira K, Kobayashi K, Toyama K, Nakamura HK, Shoji H, Takao K, Takeuchi R, Yamaguchi S, Kataoka M, Otsuka S, Takahashi M and Miyakawa T (2013) Synaptosomal-associated protein 25 mutation induces immaturity of the dentate granule cells of adult mice. *Molecular Brain* 6, 12.

Okada N, Fukunaga M, Yamashita F, Koshiyama D, Yamamori H, Ohi K, Yasuda Y, Fujimoto M, Watanabe Y, Yahata N, Nemoto K, Hibar DP, van Erp TGM, Fujino H, Isobe M, Isomura S, Natsubori T, Narita H, Hashimoto N, Miyata J, Koike S, Takahashi T, Yamasue H, Matsuo K, Onitsuka T, Iidaka T, Kawasaki Y, Yoshimura R, Watanabe Y, Suzuki M, Turner JA, Takeda M, Thompson PM, Ozaki N, Kasai K and Hashimoto R (2016) Abnormal asymmetries in subcortical brain volume in schizophrenia. *Molecular Psychiatry* 21, 1460–1466.

Oldfield RC (1971) The assessment and analysis of handedness: the Edinburgh inventory. *Neuropsychologia* 9, 97–113.

Omar MH, Campbell MK, Xiao X, Zhong Q, Brunken WJ, Miner JH, Greer CA and Koleske AJ (2017) CNS neurons deposit Laminin α5 to stabilize synapses. *Cell Reports* 21, 1281–1292.

Ota M, Sato N, Hidese S, Teraishi T, Maikusa N, Matsuda H, Hattori K and Kunugi H (2017) Structural differences in hippocampal subfields among schizophrenia patients, major depressive disorder patients, and healthy subjects. *Psychiatry Research* 259, 54–59.

Purcell S, Neale B, Todd-Brown K, Thomas L, Ferreira MAR, Bender D, Maller J, Sklar P, de Bakker PIW, Daly MJ and Sham PC (2007) PLINK: a tool set for whole-genome association and population-based linkage analyses. *American Journal of Human Genetics* **81**, 559–575.

Rhindress K, Robinson DG, Gallego JA, Wellington R, Malhotra AK and Szeszko PR (2017) Hippocampal subregion volume changes associated with antipsychotic treatment in first-episode psychosis. *Psychological Medicine* **47**, 1706–1718.

Risch N and Merikangas K (1996) The future of genetic studies of complex human diseases. *Science* **273**, 1516–1517.

Sauras R, Keymer A, Alonso-Solis A, Díaz A, Molins C, Nuñez F, Rabella M, Roldán A, Grasa E, Alvarez E, Portella MJ and Corripio I (2017) Volumetric and morphological characteristics of the hippocampus are associated with progression to schizophrenia in patients with first-episode psychosis. *European Psychiatry: The Journal of the Association of European Psychiatrists* **45**, 1–5.

Schmitt A, Steyskal C, Bernstein H-G, Schneider-Axmann T, Parlapani E, Schaeffer EL, Gattaz WF, Bogerts B, Schmitz C and Falkai P (2009) Stereologic investigation of the posterior part of the hippocampus in schizophrenia. *Acta Neuropathologica* **117**, 395–407.

Schneider CE, White T, Hass J, Geisler D, Wallace SR, Roessner V, Holt DJ, Calhoun VD, Gollub RL and Ehrlich S (2014) Smoking status as a potential confounder in the study of brain structure in schizophrenia. *Journal of Psychiatric Research* **50**, 84–91.

Schobel SA, Lewandowski NM, Corcoran CM, Moore H, Brown T, Malaspina D and Small SA (2009) Differential targeting of the CA1 subfield of the hippocampal formation by schizophrenia and related psychotic disorders. *Archives of General Psychiatry* **66**, 938–946.

Segall JM, Turner JA, van Erp TGM, White T, Bockholt HJ, Gollub RL, Ho BC, Magnotta V, Jung RE, McCarley RW, Schulz SC, Lauriello J, Clark VP, Voyvodic JT, Diaz MT and Calhoun VD (2009) Voxel-based morphometric multisite collaborative study on schizophrenia. *Schizophrenia Bulletin* **35**, 82–95.

Small SA, Schobel SA, Buxton RB, Witter MP and Barnes CA (2011) A pathophysiological framework of hippocampal dysfunction in ageing and disease. *Nature Reviews. Neuroscience* **12**, 585–601.

Steinberg S, Mors O, Børglum AD, Gustafsson O, Werge T, Mortensen PB, Andreassen OA, Sigurdsson E, Thorgeirsson TE, Böttcher Y, Olason P, Ophoff RA, Cichon S, Gudjonsdottir IH, Pietiläinen OPH, Nyegaard M, Tuulio-Henriksson A, Ingason A, Hansen T, Athanasiu L, Suvisaari J, Lonnqvist J, Paunio T, Hartmann A, Jürgens G, Nordentoft M, Hougaard D, Norgaard-Pedersen B, Breuer R, Möller H-J, Giegling I, Glenthøj B, Rasmussen HB, Mattheisen M, Bitter I, Réthelyi JM, Sigmundsson T, Fossdal R, Thorsteinsdottir U, Ruggeri M, Tosato S, Strengman E, Genetic Risk and Outcome in Psychosis, Kiemeney LA, Melle I, Djurovic S, Abramova L, Kaleda V, Walshe M, Bramon E, Vassos E, Li T, Fraser G, Walker N, Toulopoulou T, Yoon J, Freimer NB, Cantor RM, Murray R, Kong A, Golimbet V, Jönsson EG, Terenius L, Agartz I, Petursson H, Nöthen MM, Rietschel M, Peltonen L, Rujescu D, Collier DA, Stefansson H, St Clair D and Stefansson K (2011) Expanding the range of ZNF804A variants conferring risk of psychosis. *Molecular Psychiatry* **16**, 59–66.

van Erp TGM, Greve DN, Rasmussen J, Turner J, Calhoun VD, Young S, Mueller B, Brown GG, McCarthy G, Glover GH, Lim KO, Bustillo JR, Belger A, McEwen S, Voyvodic J, Mathalon DH, Keator D, Preda A, Nguyen D, Ford JM and Potkin SG, FBIRN (2014) A multi-scanner study of subcortical brain volume abnormalities in schizophrenia. *Psychiatry Research* **222**, 10–16.

van Erp TGM, Preda A, Turner JA, Callahan S, Calhoun VD, Bustillo JR, Lim KO, Mueller B, Brown GG, Vaidya JG, McEwen S, Belger A, Voyvodic J, Mathalon DH, Nguyen D, Ford JM and Potkin SG, FBIRN (2015) Neuropsychological profile in adult schizophrenia measured with the CMINDS. *Psychiatry Research* **230**, 826–834.

van Erp TGM, Hibar DP, Rasmussen JM, Glahn DC, Pearlson GD, Andreassen OA, Agartz I, Westlye LT, Haukvik UK, Dale AM, Melle I, Hartberg CB, Gruber O, Kraemer B, Zilles D, Donohoe G, Kelly S, McDonald C, Morris DW, Cannon DM, Corvin A, Machielsen MWJ,

Koenders L, de Haan L, Veltman DJ, Satterthwaite TD, Wolf DH, Gur RC, Gur RE, Potkin SG, Mathalon DH, Mueller BA, Preda A, Macciardi F, Ehrlich S, Walton E, Hass J, Calhoun VD, Bockholt HJ, Sponheim SR, Shoemaker JM, van Haren NEM, Pol HEH, Ophoff RA, Kahn RS, Roiz-Santianez R, Crespo-Facorro B, Wang L, Alpert KI, Jönsson EG, Dimitrova R, Bois C, Whalley HC, McIntosh AM, Lawrie SM, Hashimoto R, Thompson PM and Turner JA (2016) Subcortical brain volume abnormalities in 2028 individuals with schizophrenia and 2540 healthy controls via the ENIGMA consortium. *Molecular Psychiatry* **21**, 585.

Tamminga CA, Stan AD and Wagner AD (2010) The hippocampal formation in schizophrenia. *The American Journal of Psychiatry* **167**, 1178–1193.

Tamminga CA, Southcott S, Sacco C, Wagner AD and Ghose S (2012) Glutamate dysfunction in hippocampus: relevance of dentate gyrus and CA3 signaling. *Schizophrenia Bulletin* **38**, 927–935.

Uttl B (2002) North American Adult Reading Test: age norms, reliability, and validity. *Journal of Clinical and Experimental Neuropsychology* **24**, 1123–1137.

Van Leemput K, Bakkour A, Benner T, Wiggins G, Wald LL, Augustinack J, Dickerson BC, Golland P and Fischl B (2008) Model-based segmentation of hippocampal subfields in ultra-high resolution in vivo MRI. *Medical Image Computing and Computer-Assisted Intervention: MICCAI … International Conference on Medical Image Computing and Computer-Assisted Intervention* **11**, 235–243.

Van Leemput K, Bakkour A, Benner T, Wiggins G, Wald LL, Augustinack J, Dickerson BC, Golland P and Fischl B (2009) Automated segmentation of hippocampal subfields from ultra-high resolution in vivo MRI. *Hippocampus* **19**, 549–557.

Walton NM, Zhou Y, Kogan JH, Shin R, Webster M, Gross AK, Heusner CL, Chen Q, Miyake S, Tajinda K, Tamura K, Miyakawa T and Matsumoto M (2012) Detection of an immature dentate gyrus feature in human schizophrenia/bipolar patients. *Translational Psychiatry* **2**, e135.

Watanabe K, Taskesen E, van Bochoven A and Posthuma D (2017) Functional mapping and annotation of genetic associations with FUMA. *Nature Communications* **8**, 1–11.

Wheeler DW, White CM, Rees CL, Komendantov AO, Hamilton DJ and Ascoli GA (2015) Hippocampome.org: a knowledge base of neuron types in the rodent hippocampus. *eLife* **4**, 1–28.

Whelan CD, Hibar DP, van Velzen LS, Zannas AS, Carrillo-Roa T, McMahon K, Prasad G, Kelly S, Faskowitz J, deZubiracay G, Iglesias JE, van Erp TGM, Frodl T, Martin NG, Wright MJ, Jahanshad N, Schmaal L, Sämann PG and Thompson PM, Alzheimer's Disease Neuroimaging Initiative (2016) Heritability and reliability of automatically segmented human hippocampal formation subregions. *NeuroImage* **128**, 125–137.

Wisse LEM, Biessels GJ and Geerlings MI (2014) A critical appraisal of the hippocampal subfield segmentation package in FreeSurfer. *Frontiers in Aging Neuroscience* **6**, 261.

Yushkevich PA, Avants BB, Pluta J, Minkoff D, Detre JA, Grossman M and Gee JC (2008) Shape-based alignment of hippocampal subfields: evaluation in postmortem MRI. *Medical Image Computing and Computer-Assisted Intervention: MICCAI … International Conference on Medical Image Computing and Computer-Assisted Intervention* **11**, 510–517.

Yushkevich PA, Avants BB, Pluta J, Das S, Minkoff D, Mechanic-Hamilton D, Glynn S, Pickup S, Liu W, Gee JC, Grossman M and Detre JA (2009) A high-resolution computational atlas of the human hippocampus from postmortem magnetic resonance imaging at 9.4 T. *NeuroImage* **44**, 385–398.

Zhang R, Valenzuela RK, Lu S, Meng L, Guo T, Du X, Kang W and Ma J (2011) Is the conserved mammalian region of ZNF804A locus associated with schizophrenia? A population-based genetics analysis. *Schizophrenia Research* **133**, 159–164.

Zhang H, Zhang Y-W, Chen Y, Huang X, Zhou F, Wang W, Xian B, Zhang X, Masliah E, Chen Q, Han J-DJ, Bu G, Reed JC, Liao F-F, Chen Y-G and Xu H (2012) Appoptosin is a novel pro-apoptotic protein and mediates cell death in neurodegeneration. *The Journal of Neuroscience* **32**, 15565–15576.